HHS Public Access

Author manuscript

Prog Biophys Mol Biol. Author manuscript; available in PMC 2020 July 01.

Published in final edited form as:

Prog Biophys Mol Biol. 2019 July ; 144: 102–115. doi:10.1016/j.pbiomolbio.2018.07.015.

Tropomyosin Dynamics during Cardiac Muscle Contraction as Governed by a Multi-Well Energy Landscape

Yasser Aboelkassem[1] and **Natalia Trayanova**

Institute for Computational Medicine, Department of Biomedical Engineering Johns Hopkins University, Baltimore, MD, USA

Abstract

The dynamic oscillations of tropomyosin molecules in the azimuthal direction over the surface of the actin filament during thin filament activation are studied here from an energy landscape perspective. A mathematical model based on principles from nonlinear dynamics and chaos theory is derived to describe these dynamical motions. In particular, an energy potential with three wells is proposed to govern the tropomyosin oscillations between the observed regulatory positions observed during muscle contraction, namely the blocked “B”, closed “C” and open “M” states. Based on the variations in both the frequency and amplitude of the environmental (surrounding the thin filament system) driving tractions, such as the electrostatic, hydrophobic, and Ca^{2+}-dependent forces, the tropomyosin movements are shown to be complex; they can change from being simple harmonic oscillations to being fully chaotic. Three cases (periodic, period-2, and chaotic patterns) are presented to showcase the different possible dynamic responses of tropomyosin sliding over the actin filament. A probability density function is used as a statistical measure to calculate the average residence time spanned out by the tropomyosin molecule when visiting each (B, C, M) equilibrium state. The results were found to depend strongly on the energy landscape profile and its featured barriers, which normally govern the transitions between the B-C-M states during striated muscle activation.

Keywords

Tropomyosin Dynamics; Chaos Theory; Myofilament Modeling

1. Introduction

Tropomyosin (Tm) dynamical motions over the surface of an actin filament play an important role in the process of striated thin filament activation and have been hypothesized to be a key effector in regulating muscle contractions. For instance, the Tm-chain exhibits unique characteristics [1–6], which have been shown to affect the stability of the actin

[1]Dr. Aboelkassem’s current address is Department of Bioengineering, University of California San Diego, La Jolla, CA, USA. yaboelkassem@ucsd.edu.

filament and modulate its interaction with the surrounding motor proteins. Additionally, Tm has the ability to oscillate between distinct regulatory locations in response to binding of the different thin filament activators [7–9]. The dynamics of the Tm regulatory movements is believed to be complex owing to the inherent nonlinearities, flexibility, and cooperativity in the structure of the thin filament proteins and in the surrounding activation forces [10–13]. These structure determinates could allow for different parts of a Tm molecule to effectively exist in different (B-C-M) states, and a Tm molecule to influence, and be influenced by, the B-C-M state of the nearest-neighboring Tm molecules.

Tm is a coiled-coil regulatory protein that binds head-to-tail to the adjacent Tm molecules to form a continuous chain. This chain is constrained at a particular angular position slightly away from the surface of the actin filament by electrostatic forces. This setting allows Tm to oscillate in the azimuthal direction (ϕ) with respect to the longitudinal axis of actin. Therefore, Tm is generally considered to be a flexible chain, as shown by several recent myofilament mechanistic models [14–18]. These models were developed based on the path-integral theory of a continuous flexible chain [19], which was used to derive the nonlinear elastic energy governing the azimuthal movements of Tm. These models used a stochastic approach based on the standard Monte Carlo algorithm, and Tm was assumed to slide over actin, without rotating around its own axis, with an elastic energy that depends only on the bending mode/stiffness of Tm (but not the torsional stiffness). These models have successfully predicted the angular positions spanned out by the Tm-chain and regulated by Ca^{+1} availability during the process of thin filament activation. However, their applicability in describing how Tm alternates between angular locations is limited, and they cannot be used to track the intrinsic Tm dynamical motions between regulatory positions.

Currently, there are two debated hypothetical mechanisms (sliding vs. rolling) proposed to describe Tm motions on the surface of actin. The sliding mechanism suggests that Tm translates over a relatively flat region and assumes that there are no major changes in the structural configurations of either Tm or actin [9, 17, 20]. In contrast, the rolling hypothesis posits an axial rotation/deformation of the Tm-chain about its axis [21, 22]. In addition to the sliding and rolling hypotheses, D. Sousa and his co-workers have recently proposed an alternative mechanism (rocking) that might better explain the actual Tm movements specifically between the C and -M states [23]. The rocking motion model was proposed based on a detailed Cryo-EM structural study, which showed that the C- and M-states are very close to each other and therefore are likely to transition between equilibrium positions via a rocking displacement.

In all motion scenarios (sliding, rolling and rocking), the Tm-chain undergoes distinct movements to uncover the myosin-S1 binding sites located on the surface of the actin filament. These motions are characterized by three equilibrium positions, namely: the blocked position “B” (binding sites are blocked), closed position “C” (weak binding is permissible), and the open position “M” (strong binding of S1). These maneuvers are set by a well-established mechanism, commonly known as the three-state-model (B-C-M) of McKillop and Geeves [9]. While the three-state-model describes the equilibrium regulatory states of Tm, the intrinsic mechanism by which Tm-chain oscillates between these states remains incompletely understood.

Recently, Tm dynamical movements on the surface of the actin filament were explained using an “energy landscape” perspective [24–27]. Specifically, in a troponin (Tn)-free model (only F-actin and Tm being considered), reconstructions from electron microscopy experiments supplemented by computational chemistry simulations were used to predict the energy barrier between various Tm regulatory positions. Results of these studies successfully predicted the azimuthal displacements of Tm and its associated energy landscape potential, the latter shown to exhibit only a single energy minimum with a fairly broad well. Orzechowski and co-workers [26] hypothesized that, when the rest (i.e., Tn and myosin) of the myofilament structure is considered, this single-well potential landscape will deform, allowing for multiple wells with various energy barriers to form. Thus, trapping of Tm into one of the three (B-C-M) regulatory positions will be controlled mainly by energy separations between the multi-well features in the entire myofilament energy landscape.

These energy landscape results [24–27] provide a useful platform that can be used to better understand the mechanistic role of Tm dynamics during muscle activation. However, the exact spatio-temporal mechanisms governing how the Tm-chain moves over the actin surface and which energy landscape it follows remain unresolved, hindering the complete understanding of Tm dynamics. One of the important unanswered questions is whether Tm oscillates between the distinct three (B-C-M) regulatory states with simple harmonic modes, or with chaotic dynamic patterns or completely random behavior.

In this study, we propose a novel mathematical model that explains Tm dynamical motions on the surface of the actin filament using principles from nonlinear dynamical systems, chaos theory, and the recent energy landscape hypothesis/findings [24–27]. The Tm oscillations between the three observed regulatory equilibrium states (B-C-M) are modelled using energy potential with multiple wells [28]. Each well in the energy landscape profile is hypothesized to mimic one of the regulatory positions (B-C-M) proposed by the three-state-model [9]. The model assumes that switching process between these conformational states is inherently deterministic. The Jacobian and Lyapunov methods are then used to study the system’s local and global stability. A bifurcation analysis using Melinkov function is also used to find conditions (parameter values) that signify Tm transitions from simple harmonic oscillation to chaotic behaviors. We demonstrate that Tm movements over the actin surface may exhibit periodic, aperiodic, and chaotic behaviors during muscle contraction.

2. Methods

Consider the situation when the Tm molecule moves azimuthally over the surface of the actin filament during the thin filament activation process. These movements eventually lead to global conformational changes that uncover the myosin-binding sites, hence facilitating muscle contraction. In general, the equation that govern the dynamics of this motion can be derived from the momentum balance using a stochastic approach, which can be given in a non-dimensional form according to Langevin’s equation as,

$$\ddot{X} + \zeta \dot{X} + \nabla V(X) = \sum F(t) \quad (1)$$

where the superscript (·) denotes derivatives with respect to time, ∇ is the standard gradient operator, X is the activation coordinate vector, and ζ is damping coefficient. V(X) is a multi-well energy potential used to govern Tm regulatory motions between its equilibrium positions. $\Sigma\ F(t) = T(t) + N(t)$ is the total driving force vector. $T(t) = [T_r,\ T_\phi, T_Z]$ combines all the environmental forces that surrounds the thin filament and induce distinct Tm motions along the reaction coordinates. $N(t) = [N_r,\ N_\phi, N_Z]$ is a fluctuation force vector due to thermal noise, which is normally modeled by a Gaussian white noise distribution, which has a zero mean and satisfies the fluctuation-dissipation theorem,

$$< N(t) > = 0 \qquad \& \qquad < N(t)N(s) > = 2\zeta k_B T_K \delta(t-s) \quad (2)$$

where k_B, T_K, and δ are the Boltzmann constant, temperature in Kelvin, and the Dirac delta function, respectively. The present analysis extends the work by Earley [8] and generalizes his approach and hypothesis by assuming that Tm could alternate between regulatory states not only harmonically but also in a chaotic fashion. The model development is supported by the following important findings/facts from the literature; i) during thin filament activation process, Tm oscillates between three well-known equilibrium states, blocked “B”, closed “C”, and open “M” [9], ii) these Tm movements can be explained from energy landscape perspective [26,27]. The model details are given in the following subsections.

Energy landscape: Tm dynamics as governed by a three-well potential

The potential mechanical energy stored in motor proteins can be described by an energy landscape profile [29]. This interaction energy profile is normally used to find the system’s equilibrium positions and governs the motions between these positions. Moreover, according to the Lagrangian-Hamiltonian mechanics principles, the spatial gradient (derivative w.r.t the interaction coordinate) of this potential gives rise to a stiffness force term that contributes to the overall traction (inertial, damping, and external-driving) acting on the system.

In modeling Tm motion dynamics, it is well accepted that the Tm azimuthal position ϕ over the surface of actin filaments is controlled by the free Ca^{2+} concentration and the interactions between the actin filament, the troponin complex (TnC, TnI, TnT), and the myosin head sub-fragment (S1). This dynamic environment around the Tm chain is hypothesized to follow a multi-well energy landscape that governs Tm’s oscillations between the observed three-equilibria positions on the actin surface. Reconstruction of the exact topological form of this energy potential profile based on experimental data has not been possible yet, and is considered a major challenge. Instead, a pre-assumed (i.e., theoretically-based), well-posed and biophysically reasonable energy potential profile that mimics the above mentioned (B-C-M) motions is used here. Our proposed approach is given as a first step toward investigating and understanding the fundamental dynamics of the Tm complex oscillations seeking a new class of myofilament models.

Herein, we assume that the azimuthal position of Tm ϕ on the surface of actin filament is governed purely by a potential function $V(\phi)$ with three-wells. Each well is hypothesized to be consistent with the three-state model [9] and refers to one of the B-C-M positions. These distinct positions are explained as follows: (i) The blocked state “B” ($\phi = \phi_-$) refers to a

situation where the cytosolic Ca^{+2} ions are absent or very low, the troponin-T(TnT) binds to tropomyosin forming interlocking troponin-tropomyosin complex, and the troponin-I(TnI) binds to actin holding this complex in place. (ii) The closed state "C" ($\phi = \phi_o$) is formed when Ca^{+2} becomes available and binds to troponin-C(TnC). (iii) The open state "M" ($\phi = \phi_+$) is established when the myosin bind to the thin filament and forming cross-bridges and power stroke. These distinct regulatory locations and the hypothesized energy potential are schematically shown in Fig. 1 A & B respectively. An expression to this profile can be given by

$$V(\phi(t)) = \frac{1}{2}\alpha\phi^2 + \frac{1}{4}\beta\phi^4 + \frac{1}{6}\gamma\phi^6 \quad (3)$$

where, α, β, and γ are arbitrary parameters given to control the shape, the activation barriers, and the critical (stable/unstable) points of the proposed energy landscape profile. Ideally, these free parameters can be used to match the proposed profile with an experimentally reconstructed profile, when the latter becomes available. Moreover, they can be used to draw connections between the transition rates and the activation energy barriers via Gibbs relations. For example, when moving from blocked to closed states, the transition rate can be given as $k_{B^+} = exp\left(-\Delta V_{B \leftrightarrow C}/RT\right)$ where $\Delta V_{B\leftrightarrow C}$ is set by the values of α, β, and γ, respectively. However, in this study we focus on identifying the angular motions of Tm from a nonlinear dynamical point of view at a fixed energy barrier height and for a given excitation force, rather than focusing on the actomyosin chemo-mechanical (ATP Hydrolysis) process. Therefore, these parameters are kept constant.

We focus our attention on the azimuthal coordinate only and assume that fluctuations in the azimuthal direction are bounded and are much smaller than axial fluctuations. In other words, the system is assumed to be inherently deterministic rather than random [30]. Additionally, the environmental forces[8] along this direction are assumed to be smooth and slow function in time. Therefore, a deterministic mapping to the forcing term in the Langevin equation can be rewritten by replacing the Gaussian white noise with a deterministic chaotic dynamics. In other words, we are seeking a model response induced by deterministic forces only along the azimuthal direction.

The deterministic version of the Langevin equation(1) that governs the azimuthal movement of Tm on the actin's surface can be given by

$$\ddot{\phi} + \zeta\dot{\phi} + \frac{dV(\phi)}{d\phi} = T_\phi(t) \quad (4)$$

It should be emphasized that, although the system is subjected to thermal fluctuations, we have followed a deterministic modeling approach [30], which has been used previously to model ionic-channel kinetics based on chaotic theory. Since we are interested in modeling the collective dynamics of a strand of Tm molecules (one of two such strands on each thin filament where each strand is formed by Tm molecules joined "head to tail"), we represent

that structure herein by a single lumped inertial body with a total mass equal to the sum of all Tm molecules that regulate the thin filament activation. Therefore, the inertia of this lumped Tm body is assumed to be important and comparable with the damping effect, hence the inertial effect (the acceleration term) is kept in the equations. It should also be noted that the damping coefficient ζ (given in a non-dimensional form) is also an important parameter in the model and is believed to strongly influence the thin filament dynamics. For instance, experimental observations have already demonstrated a critical dependence of thin filament regulatory unit dynamics on solvent viscosity [31].

The term $\frac{dV}{d\phi}$ is included to account for the traction induced by the energy profile of the Tm body. Herein, we chose to use a non-dimensional formulation since the exact mathematical form of the driving forces is not fully known. The surrounding environmental driving tractions (forces) are given by the source term T, and are induced by the thick and thin filaments electrostatic and hydrophobic force interactions [14, 15, 32], and by the Ca^{+2}-dependent forces exerted by the Troponin-complex proteins. These external effectors can be lumped together and assumed to vary harmonically, i.e., $T_\phi(t) = T_o \cos(\omega t)$ with excitation frequency ω and amplitude T_o. Using equations (3–4), we obtain:

$$\ddot{\phi} + \zeta\dot{\phi} + \alpha\phi + \beta\phi^3 + \gamma\phi^5 = T_o \cos(\omega t) \quad (5)$$

The proposed potential profile is symmetric in shape with three wells and five critical (stable and saddle) points. Therefore, the term $\frac{dV}{d\phi}$ can be rewritten in a simplified form as

$$\frac{dV}{d\phi} = \alpha\phi + \beta\phi^3 + \gamma\phi^5 = \phi\left(\phi^2 - \phi_o^2\right)\left(\phi^2 - \phi_x^2\right) \quad (6)$$

Equation (5) can now be rewritten as

$$\ddot{\phi} + \zeta\dot{\phi} + \phi\left(\phi^2 - \phi_o^2\right)\left(\phi^2 - \phi_x^2\right) = T_o \cos(\omega t) \quad (7)$$

where, $\phi = 0, \pm\phi_o$, and $\pm\phi_x$ are the system critical points. The stable points are found to be located at $\phi = 0$ and $\pm\phi_o$. Each stable point is assigned to a tropomyosin conformational (B-C-M) state. Additionally, there are two unstable (saddle) points located at $\pm\phi_x < \pm\phi_o$, which mark and control the trapping energy barriers required for transitions between the Tm regulatory states. The stable point located at $\phi = 0$ is chosen such that it represents the closed "C" state. The other two wells are chosen to be located at $\phi_o = +1$, and represent the blocked "B" and open "M" states, respectively. The coefficients in equation (3) control the shape of the energy potential $V(\phi)$ profile and its critical points locations. By applying simple algebra manipulations, these coefficients can be related to the locations of the system critical points as: $\alpha = \phi_x^2$, $\beta = -(1 + \phi_x^2)$, and $\gamma = 1$, which renders the shape of the potential $V(\phi)$ to depend only on the locations of the saddle points $\pm\phi_x$, as shown in Fig. 2 A. It should be noted that although we are proposing a symmetric energy profile to describe

the Tm dynamics, the analysis is kept general to accommodate other complex anharmonic (i.e., deviation from being harmonic and symmetric) energy landscape profiles with variable energy barriers to account for the Ca^{+2} transients during thin filament activation.

The phase portrait ($\phi - \dot{\phi}$) for the undamped (i.e., $\zeta = 0$) and unperturbed system (i.e.,T = 0) is presented in Fig. 2B. This plot clearly shows two distinct orbits related to the saddle points, namely the homoclinic and heteroclinic manifolds. The homoclinic orbit connects each saddle point with itself, while the heteroclinic orbit connects the two saddle points to each other. These orbits are important because they form the separatrix between each energy well i.e., between Tm's conformational states. These manifolds can be very sensitive to any disturbances and/or fluctuations in the system parameters because of the inherent nonlinearities in the system. Therefore, the stability and bifurcations of both homoclinic and heteroclinic orbits are hypothesized to control the Tm's dynamical behavior and used herein to identify whether Tm behaves as a simple harmonic oscillator or moves with other possible complex chaotic patterns. Thus, a system stability analysis is required.

Local and global stability analysis

In order to determine the stability requirements of the above Tm dynamical model, equation (7) is rewritten as two ordinary differential equations in the phase plane

$$\begin{cases} \dot{\phi} = \psi \\ \dot{\psi} = -\zeta\psi - \phi\left(\phi^2 - \phi_o^2\right)\left(\phi^2 - \phi_x^2\right) + T_o\cos(\omega t) \end{cases} \quad (8)$$

To study the local and global stability, we first consider the unforced scenario (the forcing term is set to zeros i.e., T = 0),

$$\begin{cases} \dot{\phi} = \psi \\ \dot{\psi} = -\zeta\psi - \phi\left(\phi^2 - \phi_o^2\right)\left(\phi^2 - \phi_x^2\right) \end{cases} \quad (9)$$

The local stability analysis around the equilibrium points of the linearized form of the above system (Eq. 9) can be determined by firstly calculating the Jacobian matrix **J** and finding its eigenvalues. Analyses have shown that there exist three sinks (stable points); one of them is located at the origin (0,0) with eigenvalues of $\lambda = \frac{1}{2}(-\zeta \pm \sqrt{\zeta^2 - 4\phi_x{}^2})$ with $Re(\lambda) < o$, and two other points located are at $(0,\pm\phi_0)$ with eigenvalues of $\lambda = \frac{1}{2}(-\zeta \pm \sqrt{\zeta^2 - 8(1 - \phi_x{}^2)})$ with $Re(\lambda) < o$. Also, there are two saddle (unstable) points located at $(0,\pm\phi_x)$. The corresponding eigenvalues at the saddle points are $\lambda = \frac{1}{2}(-\zeta \pm \sqrt{\zeta^2 - 8\phi_x{}^2(1 - \phi_x{}^2)})$. The corresponding eigenvalues at the saddle points are $\lambda = \frac{1}{2}(-\zeta \pm \sqrt{\zeta^2 - 8\phi_x{}^2(1 - \phi_x{}^2)})$.

Furthermore, the global stability of the system can be obtained by calculating the Lyapunov function *L*, which should be positive definite for a globally stable system. In our proposed Tm-dynamical system model, Lyapunov function can be obtained easily since the system is

Hamiltonian H and having a total energy (kinetic and potential) that is equal to L. Lyapunov function for the above system can be given as

$$L = H = \frac{1}{2}\psi^2 + \frac{1}{2}\phi_x^2\phi^2 - \frac{1}{4}\left(1 + \phi_x{}^2\right)\phi^4 + \frac{1}{6}\phi^6 \quad (10)$$

Differentiating the above expression for L with respect to time and using equation (9) yields $\dot{L} = -\zeta\psi^2$, which is always negative for positively damping coefficient i.e., $\zeta > 0$ and for non-zero velocity i.e., $\psi \neq 0$. This analysis suggests that the global solutions to the present system are always stable (bounded) for any choice of system parameters, provided that the system is not driven by external forces i.e., T = 0. However, linearized theory analysis suggests that, the system is still globally bounded for a small forcing amplitude T_o. Owing to the fact that the thin filament is composed of complex structures of multi-subunit machinery proteins that interact with each other in a nonlinear fashion, Tm can exhibit a multitude of dynamical responses such as for instance periodic, aperiodic, chaotic, or even behave in a completely random fashion. Therefore, it is important to determine a set of criteria that identify the possible responses of the Tm dynamical system. Melnikov's function [33] is the approach that we follow to find the conditions which mark transitions to chaos or other aperiodic system responses.

Conditions for bifurcation and chaotic motions

Nonlinear systems are in general sensitive to fluctuations in the main model parameters. In our analysis, parameters such as the damping coefficient ζ, excitation frequency ω, and driving amplitude T_o are expected to have influence on the Tm transitions from one position to another and its general dynamical responses. In order to study the effects of these parameters, Melnikov [33] theory is used to find bifurcation conditions and transitions to chaos [34]. Melnikov function M is considered to be a fundamental theory in bifurcation analysis and commonly used tool in nonlinear dynamics studies to determine the existence of chaos induced by a small perturbation to a smoothed Hamiltonian system, similar to the one derived in this study. In this theory, a first order approximation is used to determine the distance between the stable and unstable manifolds of the perturbed system. This makes it possible to find the criteria for the existence of transverse intersection points in the sense of Poincare' maps, which imply the existence of fractal basin boundaries and thus a "horseshoes" structure of chaos.

To derive the criteria for the onset of chaos in our model, we use the Melnikov function M along with the Hamiltonian H expression given by equation (10). The first step in this analysis is to find expressions for both homoclinic (orbits that connect each saddle point to itself) and heteroclinic (orbits that connect two saddle points) trajectories. Therefore, we consider the unforced system given previously by equation (9). Let $\zeta = \epsilon\hat{\zeta}$, with $0 \leq \epsilon \leq 1$, and drop ($\hat{}$) for convenience

$$\begin{cases} \dot{\phi} = \psi \\ \dot{\psi} = -\epsilon\zeta\psi - \phi\left(\phi^2 - \phi_o^2\right)\left(\phi^2 - \phi_x^2\right) \end{cases} \quad (11)$$

Considering the unperturbed system (i.e., $\epsilon = 0$), expressions for both homoclinic and heteroclinic orbits [34] can be derived and given respectively as

$$(\phi, \psi)_{ho} = \left(\pm \frac{\sqrt{2}\phi_x \cosh(\frac{f_1 t}{2})}{\sqrt{f_2 + \cosh(f_1 t)}}, \pm \frac{\sqrt{2} f_1 \phi_x f_1 (f_2 - 1)\sinh(\frac{f_1 t}{2})}{2(f_2 + \cosh(f_1 t))^{\frac{3}{2}}} \right) \quad (12)$$

$$(\phi, \psi)_{he} = \left(\pm \frac{\sqrt{2}\phi_x \sinh(\frac{f_1 t}{2})}{\sqrt{-f_2 + \cosh(f_1 t)}}, \pm \frac{\sqrt{2} f_1 \phi_x f_1 (1 - f_2)\cosh(\frac{f_1 t}{2})}{2(-f_2 + \cosh(f_1 t))^{\frac{3}{2}}} \right) \quad (13)$$

where f_1 and f_2 are functions of the stable ($\phi = \pm\varphi_x$) and saddle ($\varphi = \pm \varphi_x$) points, which can be identified using the potential landscape used in the model. These functions can be given as $f_1 = \phi_x{}^2\sqrt{2\gamma\left(f_3{}^2 - 1\right)}$ and $f_2 = \frac{5 - 3f_3{}^2}{3f_3{}^2 - 1}$ where $f_3 = \frac{\phi_o}{\phi_x}$, and $\gamma = 1$ is the coefficient of the ϕ^6 term in our prescribed potential. The "±" sign refers to the separatrix manifold which separates two orbits in phase space plane. In order to derive a condition for the onset of chaotic response, the perturbed system (i.e., $\epsilon \neq 0$) is considered, and we apply again the Melnikov function for both the homoclinic and heteroclinic orbits

$$M(t^*)_x = \int_{-\infty}^{\infty} (-\zeta\psi_x{}^2 + T_o\psi_x \cos(\omega(t - t^*)))dt \quad (14)$$

where the subscript (x = ho or he) stands for being either on a homoclinic or a heteroclinic trajectory. A homoclinic or heteroclinic bifurcation occurs when $M(to)_x$ has a simple zeros and changes its sign. Using first order approximation, the Melnikov function can be obtained. The calculations lead to the following conditions for appearance of fractal basin boundaries and hence onset of chaotic responses. For the homoclinic orbit, i.e., cases at which Tm moves into the "B" or "M" state, we have

$$T_o \downarrow_{ho} \geq \left| \frac{\zeta\phi_x f_1^2}{32\omega\pi(f_2 + 1)\sin(2\omega/f_1)} \left(\frac{2f_2 + 1}{\sqrt{1 - f_2^2}} \arcsin(f_2 - \pi/2) + (f_2 + 2) \right) \right| \quad (15)$$

while for the heteroclinic orbit, i.e., the case in which the Tm moves into the middle-well "C-state", we have

$$T_o \downarrow_{he} \geq \left| \frac{\zeta \phi_x f_1^2 \sinh(2\omega/f_1)}{8\omega\pi(f_2+1)} \left(\frac{2f_2+1}{\sqrt{1-f_2^2}} \arcsin(f_2+\pi/2) + (f_2+2) \right) \right| \quad (16)$$

In the above conditions, equal signs indicate the onset of bifurcations for both homoclinic and heteroclinic trajectories. The critical values derived from these conditions at a given damping ζ can serve as a guide to estimate the parameters range at which the system undergoes transition to chaotic response. These conditions are depicted in Fig.3 A&B in both the (ω - T_o) and (ζ - T_o) planes respectively. The onset of chaotic behavior occurs in the parameter range above the homoclinic and heteroclinic bifurcations curves.

Numerical simulations

We next investigated, using numerical simulations, the sensitivity of the system to model parameters and used the analysis to reveal the inherent dynamic behavior of the system. The parameters and their associated value ranges that are responsible for inducing chaotic responses were determined as follows: The analytical expressions derived above were used to conduct numerical simulations of the Tm dynamical system described by equations (8). Specifically, we have used grids composed of 50 × 50 points in both (ω, T_o) and (ζ, T_o) planes to study the system responses. The bifurcation bounds obtained analytically and given by the inequality equations (15–16) were used as a guide to examine both periodic and aperiodic responses. Additionally, at each grid point we calculated the Lyapunov exponent to determine the onset of chaos. A system is chaotic if and only if the Lyapunov exponent attains a positive value i.e., all neighboring motions diverge exponentially from the equilibrium points.

The governing equations (8) were then integrated in time to study all possible Tm dynamic responses when it moves over actin surface during the thin filament activation process. In all studied cases herein, the system was assumed to be driven harmonically by the environmental/surrounding forces induced by the interactions between the myofilament proteins. These forces represent the thick filament electrostatic forces, thin filament hydrophobic forces, and Ca^{2+}-dependent activation forces associated with the Tn-complex. The initial conditions were chosen such that Tm was assumed to reside in the closed "C"-state and had zero angular velocity. In other words, at t = 0, φ and ψ were set to zeros for all the simulated cases. A fixed time step dt = $1/f_s$ and a sampling frequency f_s = 1000 Hz were used. We run multiple cycles (N =10000), each cycle having a period T = $2\pi/\omega$. The first 3000 cycles were ignored in the analysis to avoid transient effects. Data were analyzed using time series, frequency response, and phase portrait approaches, as well as the Poincare' maps, a well-known technique to characterize the behavior of dynamical systems in the two-dimensional phase plane. In our analysis, the Poincare' section was first chosen to satisfy the condition ((ϕ, ψ, t)| t(mod T) = t_o). The Poincare' map was then obtained by finding the intersections of solutions of the forced system with the Poincare' section, which was then used to classify the system responses. For instance, if motion is periodic, then its Poincare'

map shows only a finite number of points (a single point corresponds to a period-1 behavior; 2 points correspond to period-2 motions, etc.). However, when motion becomes chaotic (non-periodic but bounded responses), the corresponding Poincare' map contains infinite number of points. Results that highlight these scenarios in the context of Tm motions are provided below.

3. Results

The analytical expressions (Eqs. 15–16) that describe the system's bifurcations were firstly used to identify parameter ranges where periodic and aperiodic behaviors take place. Because of the low order approximation used in the analytical derivation, it cannot be used to exactly locate points where chaos occurs. Therefore, we next complemented the analytical study with numerical simulations to validate the analytical results and to explore a wide range of the system responses, including chaotic motions. Results from these parameter sweeps in the (ω - T_o) and (ζ - T_o) planes are plotted in Fig. 3 for three values of ϕ_x = 0.4, 0.5, 0.6 respectively. The "+" symbol indicates the occurrence of chaos. These were obtained by using Poincare' maps after many forcing cycles and ignoring the transient phases. The solid lines in this figure mark the border between regions of periodic and aperiodic responses.

The overall system behavior were found to strongly depend on the damping coefficient ζ, excitation frequency ω, and amplitudes T_o of the driving force. Therefore, three cases, namely periodic, period-2, and chaotic oscillations are presented below (only for ϕ_x = 0.5) to demonstrate that Tm dynamics can exhibit a wide range of dynamical responses during its motions over the surface of the actin filament.

Periodic motions

Here, we show that Tm can oscillate between the B-C-M states in a periodic fashion during the process of thin filament activation. This particular behavior has found to takes place only at specific system parameters. For instance, when the forcing frequency, amplitude, and damping coefficient are chosen to be ω = 0.5, T_o = 0.1, and ζ = 0.3, a global periodic response is observed. The time series response for the Tm's angular positions φ over a few cycles and after ignoring the transient cycles is shown in Fig.4 A. The inset on the top offers a closer look at the response signal and is given to show the system's periodicity. The frequency response shows a single peak at ω = 0.5, which is identical to the driving (excitation) frequency, as shown in Fig. 4B . The system's phase portrait is shown in Fig. 4C . This portrait suggests that if Tm is initially located in the closed "C" state, after transient cycles, Tm converges to or lands onto a periodic orbit. This periodic orbit is characterized by a limit cycle oscillations with frequency equal to the actuation/driving force frequency. The Poincare' map is shown in Fig. 4D. Clearly, there is only a single point in the map, which indicates that the system exhibits a period-1 dynamics. These results imply that Tm could move between the regulatory positions on the surface of actin filament in a periodic manner and behave globally as a simple harmonic oscillator.

Period-2 dynamics

The second scenario results are provided to show that Tm can also move over the actin surface with two distinct frequencies, fundamental and super-harmonic, and thus undergo period-2 dynamics. The parameters for this case are found to be $\omega = 0.2$, $T_o = 0.24$, and $\zeta = 0.3$. Results of simulations are depicted in Fig. 5. The time series for the Tm position is shown in Fig. 5 A for multiple cycles. The inset at the top shows the quasi-periodicity response. In Fig. 5 B, we depict the frequency content of the time series signal; two peaks located at $\omega = 0.2$ and 0.4 are observed. The first frequency corresponds to the system's fundamental harmonic frequency, which is equal to the system's forcing frequency. The second frequency represents the super-harmonic feature of the system. The frequency response indicates that the Tm chain could deviate from being a simple harmonic oscillator and behave in aperiodic fashion with super-harmonic frequencies. The corresponding phase portrait is presented in Fig. 5 C showing that Tm could oscillate locally around both B and M wells with a super-harmonic frequency, then alternate between both states with the fundamental frequency. The period-2 behavior is rendered in the Poincare' map is shown in Fig. 5 D. Two points exist in the map, showing that the system obeys a period-2 dynamical response, implying that Tm motion repeats itself exactly every two periods that are set by the external environmental forces.

Chaotic behaviour

Finally, we show a situation where Tm movements exhibit chaotic (non-periodic but bounded) oscillations over the actin surface. Based on parameter sweeps, the following forcing parameters and damping coefficients are obtained for this case: $\omega = 0.75$, $T_o = 0.25$, and $\zeta = 0.3$. The time series for the Tm positions ϕ is shown in Fig. 6 A. The inset at the top of this figure provides a closer look at the signal and clearly shows a bounded yet non-periodic response known as chaotic behavior. This chaotic response suggests that Tm movements can be altered by small changes in its initial configurations or in the surrounding driving forces. The frequency response for this scenario is presented in Fig. 6 B, which shows that the Tm dynamic in this case is characterized by multiple subharmonics preceding the fundamental frequency $\omega = 0.75$. This suggests that Tm could switch between its conformational states with various frequencies. In the phase portrait that is presented in Fig. 6 C, one can clearly see that motions for this particular set of conditions are indeed chaotic. The corresponding Poincare' map has multiple points that form a Duffing-like "horseshoe" chaotic pattern, as shown in Fig. 6 D.

Results from the cases examined above suggest that Tm sliding motions over the surface of actin filament during activation might not be simple harmonic oscillations, as suggested by Earley [8], but also could be more complex and exhibit long-term persistent chaotic responses. Furthermore, Tm can have different residency time at a specific conformational (B-C-M) state. The residency metric is controlled by the Tm dynamic motions in response to surrounding forces. The calculation of the probability density function of Tm's residency in each state is provided in the next subsection.

The effects of ϕ_χ on the Tropomyosin motions

Here we investigate the effects of varying ϕ_o on Tm dynamical motions. A numerical simulation protocol similar to the above was employed for different values of ϕ_x = 0.4, 0.5, 0.6. The time series responses for the Tm's angular positions ϕ over a few cycles are shown in Fig. 7 A for periodic, period-2, and chaotic cases. Results show that when Tm moves as a simple oscillator, ϕ_x has no effect on its behavior. However, this changes when Tm moves with period-2 or in chaotic manner, where ϕ_x plays a role in the motion responses. A comparison between the phase portrait and the Poincare' maps for each ϕ_x value is presented in Fig. 7B. These results suggest that ϕ_x can affect Tm's chaotic behavior as it alternates between the three equilibrium states. Furthermore, the locations of the saddle (unstable) points are different for different values of ϕ_x, which eventually can influence the onset of aperiodic or chaotic motions. We conclude that although all the potential profiles used herein were symmetric, the locations of the unstable points can nonetheless control the dynamics of the Tm movements.

Tropomyosin residency in the B-C-M states

The probability distribution function (PDF) for the Tm's angular position ϕ is calculated in order to estimate how often Tm resides in one of its conformational B-C-M states. The procedure for these calculations is summarized in the following steps. First, the response of the angular displacement ϕ is divided into three regions that mark each state: i) the first region ($R_1 : min \leq \phi < -0.5$) represents a situation where Tm resides in blocked "B" state, ii) the second region ($R_2 : -0.5 \leq \phi \leq 0.5$) corresponds to Tm being located in the closed "C" state, iii) The third region ($R_3: 0.5 < \phi \leq max$) represent the case when Tm is located in the open "M" state. Second, after ignoring transient effect, the time-series data are used to score the residence time interval occupied by each B-C-M state within each cycle.

The collected residency scores are then averaged over the entire number of cycles. The PDF for all the three studied cases, periodic, period-2, and chaotic dynamics, is shown in Fig. 8A for ϕ_x = 0.4, 0.5, 0.6 respectively. Results demonstrate that, in both periodic (i.e., ω = 0.5) and period-2 (i.e., ω = 0.2) cases, the PDF profiles have distinct two quasi-Gaussian distributions over the "B" and "M" states and flat distribution over the "C" state. In the third case, when the chaotic scenario is considered, these Gaussian-like peaks are smeared out, suggesting that Tm has equal tendency to reside in any of the three states. It should be noted that, these results are strong function of the proposed energy landscape profile, and are expected to vary when other potentials with Ca^{2+}-dependent energy barriers are used.

The PDF are also used to estimate the residence probability P_x occupied by each state, using numerical integration over each regulatory interval as follows

$$P_x = \int_{[\phi_x]} PDF(\phi) d\phi, \qquad x = B, C, M \quad (17)$$

where, $[\phi_x]$ represents an integration interval (the residency borders) assigned to each state. For instance, to calculate the probability of Tm residing in the "C" state, we use an interval

bounded by $\phi_C \in [-0.5, 0.5]$. Similarly, for "B" and "M" states, the intervals are chosen such that $\phi_B \in$ [min, −0.5), and $\phi_M \in$ (0.5, max] respectively. Integration is performed using the quadrature rule subject to the condition; $\Sigma\ P_X = 1$.

In Fig. 8B , we show the residence probability calculations for the three simulated cases. In the periodic (period-1) case, results demonstrate that Tm has about 40% probability to reside in the "C" state compared to that of about 30% for both "B" and "M" states. Therefore, if Tm undergoes simple harmonic oscillations, there will be high tendency to slide into the blocked "B" state or into the open "M" state with equal probability. This is valid for all the simulated cases for different ϕ_X values, which confirm that ϕ_X has no effect on the Tm dynamics when moving as a simple oscillator. These results are consistent with the time series shown in Fig. 7A.

In the period-2 case, when $\phi_X = 0.4$ is used, Tm has about ∽18% probability to reside in the "C" state, ∽34% in the "B" state, and ∽48% in the "M" state. In this particular scenario, Tm will be trapped in the "M" state with higher affinity. Finally, when the chaotic case is considered, results have shown that Tm has almost equal residency probability for residing in any of the (B-C-M) conformational states. It should be noted that for scenarios other than periodic responses, these distributions can be changed by changing the locations of the saddle points; this can be accomplished by using different values of φ_χ, or when using asymmetric energy landscape profiles.

Although, it is difficult to draw clear, exact and direct connections between the predicted Tm dynamical patterns and the various muscle contraction under physiological circumstances. The results shown in Figs. 7 & 8 suggest that Tm motions over actin surface could follow different complex oscillatory mechanisms. These Tm dynamics are then expected to regulate, for instance, both force - Ca^{+2} sensitivity and twitch characteristics. Moreover, under disease (e.g., myofilament point mutations) conditions, these dynamical patterns could be altered in a way such that they can strongly affect the thin filament activation process.

Ca^{2+}-dependency and asymmetric representation of the energy landscape profile

In this part, we show a possible extension of our approach to include Ca^{2+}-dependency, thus expanding our model capability. We hypothesize that during the thin filament activation process, the energy landscape barriers that control the Tm motions vary dynamically with the cytosolic Ca^{2+} availability. Moreover, this potential profile could also account for the possible symmetry breaking as Tm moves between equilibrium positions on the actin surface. The hypothesis is shown schematically in Fig. (9) A, where P {·} is the probability of being in one of the B-C-M states. This Ca^{2+}-dependent and asymmetric energy landscape profile can be prescribed as

$$V_{Asym}(\phi(t)) = \alpha\phi^2 - \mu\left(Ca^{2+}, n_H, Ca_{50}\right)\phi^3 + \beta\phi^4 + \gamma\phi^6 \quad (18)$$

where α, β and γ are arbitrary coefficients that denote the locations of the landscape critical points. μ is a Ca^{2+}-dependent "activation coefficient" that is used herein to break the

symmetry of the energy profile, Eq.(1). This activation coefficient is assumed to be governed by a Hill-type equation, such as

$$\mu\left(Ca^{2+}\right) = \frac{Ca^{n_H}}{Ca^{n_H} + Ca_{50}^{n_H}} - \frac{1}{2} \quad (19)$$

where n_H and Ca_{50} refer to the Hill's index and the half activation, respectively. It should be noted that, for the half activation condition, μ reaches zero and the energy profile becomes symmetric, Eq.(1). The distribution of the activation coefficient μ as a function of the Ca concentrations pCa (pCa = - $\log_{10}(Ca)$, with Ca measured in [μM]) for different Hill indices is shown in Fig. (9)B. Similarly, in Fig. (10) we show the variations of the asymmetric energy landscape as a function of pCa values. As illustrated, the energy barriers are dynamically variable, mimicking the role of Ca^{+2} during thin filament activation. For instance, when Ca^{+2} concentration is low (pCa = 7), the energy barrier ($\Delta V(\phi)_{B\rightarrow C}$) for the B-attractor is the lowest among the states, so that Tm covers the myosin head-binding sites on the actin surface, suggesting an inactivation state as shown by the point (A) in Fig. (10). As Ca^{+2} rises (pCa = 6–4), this energy barrier evolves to facilitate the Tm transition to the C-state, as shown by the points (B, C and D). At high Ca^{+2} (pCa = 3), the energy barrier ($\Delta V(\phi)_{C\rightarrow M}$) associated with the M-state becomes the lowest, facilitating Tm residency between F-actin groves. Under this condition, a full activation (i.e., M) -state is obtained and stronger twitches are produced (see point (E) on the same graph).

The Ca^{+2}-dependent (asymmetric) energy landscape hypothesis offers a more biophysically-realistic model, which can be further extended to construct a complete myofilament model, which is beyond the scope of this paper. Finally, it should be noted that the α, β and γ coefficients are arbitrary and can be used as fitting parameters to further control the energy profile's critical points, hence producing an experimentally testable model.

DISCUSSION

In the last two decades, significant efforts have been dedicated to resolve the structural components of Tm and its dynamical motions over the actin surface, aiming to better understand its role during muscle contractions [1, 24, 35–43, 43–46]. Results from these studies suggest that individual Tm molecules have low affinity to actin, however the affinity is increased when Tm molecules are connected together to form a continuous chain that wraps around the actin filament [47–49] Also, Tm floats at a distance of 8–12 $A°$ from the actin's surface, controlled by electrostatic forces [37, 50, 51]. These structural settings grant Tm the opportunity to oscillate in the circumferential direction when activated in response to the surrounding biochemical effectors [52, 53].

Energy landscape is a dynamical approach which has been proposed recently to explain Tm motions over the surface of actin filaments during activation [24–27]. Orzechowski and his colleagues [26] contemplated the impact of the observed Tm's movements on the thin filament activity using energy principles. This has been primarily accomplished by examining the Tm-actin potential profile determined from in-vitro solution studies and

supported by in-silico computational simulations. They have found that: i) in the absence of troponin-complex and myosin, Tm follows an energy landscape with a single-well. This potential has a fairly broad shape with a distinct minimum and there is no an “obvious” low energy barriers that connect the regulatory states of the filament to each other. ii) Trapping Tm in the blocked “B”, closed “C”, and open “M” positions will requires additional structural and energetic input from the binding of troponin and myosin, which is expected to deform the Tm-actin energy landscape.

Because of the exact topology (e.g., energetic barriers, shape asymmetry, and bias between equilibrium points) of the energy landscape profile that governs the mutual interactions between the thin filament regulatory proteins is not fully known yet. In this study, we have attempted to formulate and extend the work in [24–27] using mathematical modeling. A generic energy landscape potential that mimics the well-established Tm’s regulatory states is proposed. Our modeling strategy has been built on the basis of the remarkable findings above [26] and has extended the singlewell energy potential via the introduction of a three-well energy landscape to account for the existence of and energy inputs from the surrounding proteins. Additionally, the proposed energy profile is hypothesized to mimic the existence of the B-C-M regulatory positions, which are used in our analysis as stable equilibrium points.

Although we used a pre-assumed energy profile, our analysis was kept general to accommodate any biophysically detailed or “realistic” energy profile that might emerge from in-vitro experimental studies of the entire complex of myofilament regulatory proteins. A realistic energy landscape would imply finding an experimentally-based and anharmonic potential profile with non-equal energy barriers (asymmetry profile), the latter governing the transition processes between the observed regulatory states. Additionally, this profile should be dynamically variable and depending strongly on the Ca^{+2} availability in the cytosol. An example of our hypothesis to this realistic/asymmetric energy landscape as a function of Ca^{+2} is given by equation 18 and shown in Fig. 10.

Moreover, both the shape and the properties of any realistic energy landscape are expected to be sensitive to mutations expressed in the myofilament proteins, hence Tm dynamics could be altered by these mutations. Orzechowski and his colleagues [26, 27] explained the direct influence of mutations on Tm motions using the energy landscape hypothesis. Although they focused on the Tm-actin system (i.e., troponin free model), their results showed that the energy landscape approach is a promising tool to assess the effects of several Tm mutations, and thus it can be used-principles to potentially relate the initial stages of myopathy to changes in thin filament stability and regulation as it is governed by a healthy or distorted energy profile. The relationships between mutations, Tm dynamics, and energy landscape could add important characteristics to our energy landscape-based model, which it can be extended to study these inter-relationships via the nonlinear potential function term $\nu(\phi)$.

Our results suggest that Tm could alternate between its equilibrium positions not only as a simple harmonic oscillator, but also chaotically. These motion responses are controlled mainly by the energy profile morphology and the surrounding activation forces. The prescribed potential profile $\nu(\phi)$ has chosen such that it has equal potential energy barriers to

avoid biasing the system response toward a specific state rather than having equal probability of being or visiting all the states. For instance, although we have used a symmetric energy profile, which theoretically should guide Tm to have equal occupancy of being trapped in either “B” or “M” states. However, due to the system complexity, Tm’s dynamical behaviors spanned out various responses such as periodic, period-2 and chaotic oscillatory motions between its equilibrium positions.

The different oscillatory behaviors of Tm are controlled predominantly by the nonlinearity (expressed here via the multi-well energy landscape) in the system and the degree of fluctuations in the surrounding driving forces. An inquiry into the character of these motions can enhance our mechanistic understanding of the role of Tm in muscle contraction. Specifically, if Tm moves in a periodic manner, its residence time (state-occupancy) in both blocked and open states would be equal. This suggests that, for small amount of non-linearity and the driving force amplitude, Tm could switch between its equilibrium states as a simple harmonic oscillator.

When Tm moves with a period-2 dynamics or chaotically, the residence time in one of these states can significantly vary depending on the perturbations in the environmental forces surrounding the thin filament system. It should be noted that the residence time associated with each oscillatory behavior depends strongly on the energy landscape topology i.e., whether it is symmetric or asymmetric. Furthermore, depending on the surrounding fluctuations in the force magnitudes and frequency, Tm could changes its dynamical motions accordingly, within the same contraction cycle. For instance, it can start to move as a simple harmonic oscillator and then can change to a chaotic movement during the rest of the contraction cycle.

The results presented here could be useful in explaining recent experimental Cryo-EM structural data [23, 46], thus enhancing our mechanistic understanding of the Tm motions during thin filament activation. For instance, the recent experimental (Cryo-EM) study by [23] has suggested that there are two different mechanisms explaining the trajectory of Tm as it moves between the C- and M-state positions. According to the first one, Tm moves across the F-Actin face from the B-state position, past its binding site in the M-state to the C-state position, and then slides back into the tightly bound configuration where it binds to myosin, i.e. the M-state. The second mechanism hypothesizes that Tm slides from the B-state to the C-state, where tight myosin binding is blocked by steric interactions between myosin and Tm. Upon a slight rotation around the Tm helix that remains bound to F-Actin, Tm rocks over to facilitate myosin binding.

This experimental data can be qualitatively explained by our model based on the energy landscape framework as follows: For the first mechanism, starting from the B-state equilibrium position and upon activation, Tm might gain a very high potential energy which causes Tm to slide over a manifold with a large momentum passing through the M-state, i.e., without settling at that state. At this point, Tm losses momentum and jumps on another orbit with a lower energy level that eventually results in landing at the C-position, and then slides back to the M-state seeking equilibrium, where energy is minimized. This motion can symbolically be given by (**B**-C-M-**C**-**M**), where the nonbold letters refer to the “skipping”

positions on the actin while Tm is trying to reach equilibrium. This behavior is not a periodic motion but rather falls within the chaotic behavior suggested here. For the second motion mechanism, “C-M Rocking, [23]”, transition between B and C states can be done via normal sliding motion with various dynamics. However, owing to geometric constraints (C and M are very close to each other), the transition from C to M states can only fall within the periodic behavior, hence Tm moves between C and M as a simple harmonic oscillator. This can be tested by designing an energy landscape with C and M equilibrium positions that are close to each other relative to their distance to the B position. Overall, in the two scenarios, our results and the Cry-EM data suggest that Tm moves between its conformational states with various dynamical behaviors.

Despite being difficult to draw an exact connection between the predicted Tm dynamical patterns and the myofilament contraction under various physiological circumstances. Our results suggest that Tm motions over the actin surface could follow different complex oscillatory patterns. These Tm dynamical patterns are expected to play a major role in regulating, for instance, both the force - Ca^{+2} sensitivity and the twitch characteristics. Moreover, under disease (e.g., myofilament point mutations) conditions, these dynamical patterns could be altered in a way such that they can strongly affect the thin filament activation process.

In conclusion, this study provides, for the first time to the best of our knowledge, a simplified mathematical model to study Tm oscillations over the surface of actin filaments during muscle activation using nonlinear dynamics and chaos theory. The present analysis is expected to be useful in better understanding the dynamics of the Tm motions from an energy landscape perspective [26,27]. Furthermore, this model can be developed further to draw connections between Tm dynamics, energy landscape morphology, and the related cardiomyopathies.

MODEL LIMITATIONS AND POSSIBLE EXTENSION

The main focus of the present study was to develop a mathematical model that can describe the Tm dynamics over the surface of actin filament during muscle contraction rather than to study the usual myofilament’s mechanical (i.e., predicting force-Ca^{2+} sensitivity and/or twitch dynamics) properties. In order to gain a basic understanding of the Tm nonlinear dynamical behavior when governed by a multi-well energy potential, the Langevin equation was simplified by replacing the fluctuations term with a deterministic form of the driving forces. However, the analysis could be extended to include stochasticity owing to the surrounding fluctuations using the Brownian ratchet theorem.

The model does not include the Tm flexibility and cooperativity that allow for different parts of a Tm molecule to possibly exist in different (B-C-M) states, and a Tm molecule to influence, and be influenced by, the B-C-M state(s) of the nearest-neighboring Tm molecules [5, 10–12]. Therefore, the governing equations in this study were derived only for a single thin filament regulatory unit (RU: Tm-Tn-A_7), which is normally composed of a single Tm, a single Tn-complex and 7-actin’s monomers and lacks flexibility and cooperativity of activation seen in full length filaments. To overcome this limitation and to account for nearest-neighboring interactions between RUs due to Tm-Tm overlap, the

present model could be extended by writing a coupled system of equations for all the RUs in the thin filament. Normally 26 RUs are used to spatially resolve the thin filament, see [54–56].

Finally, with these possible extensions (stochasticity and spatially coupled 26-RUs) the present model permit a more complete representation of myofilament dynamic based on the energy landscape and principles of nonlinear dynamics and chaotic theory.

Acknowledgement

The authors acknowledge Dr. Anthony Cammarato, Johns Hopkins University for his insightful discussions and Dr. Andrew D. McCulloch, University of California San Diego for his expert feedback on the final draft of this study.

The authors gratefully acknowledge funding from the Leducq Foundation Network of Excellence grant Repolarization HeterogeneitY imaging for personalized Therapy of Heart arrhythmia. This work was supported in part by the National Institutes of Health (NIH) awards DP1 HL123271 and R01HL103428.

References

[1]. Hitchcock-DeGregori SE, Tropomyosin: function follows structure, Adv Exp Med Biol. 644 (2008) 60–72. [PubMed: 19209813]

[2]. Lehman W, Craig R, Tropomyosin and the steric mechanism of muscle regulation, Advances in Experimental Medicine and Biology 644 (2008) 95–109. [PubMed: 19209816]

[3]. Gunning P, O'neill G, Hardeman E, Tropomyosin-based regulation of the actin cytoskeleton in time and space, Physiol Rev. 88 (2008) 1–35. [PubMed: 18195081]

[4]. Wang C-L, Coluccio LM, New insights intothe regulation of the actin cytoskeleton by tropomyosin, Int Rev Cell Mol Biol 281 (2010) 91–128. [PubMed: 20460184]

[5]. Li XE, Holmes K, Lehman W, Jung H, Fischer S, The shape and flexibility of tropomyosin coiled coils: Implications for actin filament assembly and regulation, J Mol Biol 395 (2010) 327–339. [PubMed: 19883661]

[6]. Zheng W, Barua B, Hitchcock-DeGregori SE, Probing the flexibility of tropomyosin and its binding to filamentous actin using molecular dynamics simulations, Biophys. J. 105 (2013) 1882–1892. [PubMed: 24138864]

[7]. Phillips GN., Fillers JP, Cohen C, Motions of tropomyosin. crystal as metaphor, Biophys J 32 (1980) 485–502. [PubMed: 7248457]

[8]. Earley JJ, Simple harmonic motion of tropomyosin: proposed mechanism for length-dependent regulation of muscle active tension, Am J Physiol. 261 (1991) C1184–95. [PubMed: 1767819]

[9]. McKillop DFA, Geeves MA, Regulation of the interaction between actin and myosin subfragment 1: Evidence for three states of the thin filament, Biophys. J. 65 (1993) 693–701. [PubMed: 8218897]

[10]. Regnier M, Rivera AJ, Wang C-K, Bates MA, Chase PB, Gordon AM, Thin filament near-neighbour regulatory unit interactions affect rabbit skeletal muscle steady-state force-ca2+ relations, J. Physiol. 540 (2002) 485–497. [PubMed: 11956338]

[11]. Loong CKP, Zhou H-X, Chase PB, Persistence length of human cardiac α-tropomyosin measured by single molecule direct probe microscopy, PLoS ONE 7 (2012) e39676. [PubMed: 22737252]

[12]. Loong CKP, Badar MA, Chase PB, Tropomyosin flexural rigidity and single ca2+ regulatory unit dynamics: implications for cooperative regulation of cardiac muscle contraction and cardiomyocyte hypertrophy, Front Physiol 3 (2012) 80. [PubMed: 22493584]

[13]. El-Mezgueldi M, Tropomyosin dynamics, J Muscle Res Cell Motil 35 (2014) 203–210. [PubMed: 24510226]

[14]. Smith D, Maytum R, Geeves M, Cooperative regulation of myosin-actin interactions by a continuous flexible chain i: Actin-tropomyosin systems, Biophys. J. 84 (2003) 3155–3167. [PubMed: 12719245]

[15]. Smith D, Geeves M, Cooperative regulation of myosin-actin interactions by a continuous flexible chain ii: Actin-tropomyosin-troponin and regulation by calcium, Biophys. J 84 (2003) 3168–3180. [PubMed: 12719246]

[16]. Geeves MA, Griffiths H, Mijailovich S, Smith DA, Cooperative [ca^{2+}]-dependent regulation of the rate of myosin binding to actin: solution data and the tropomyosin chain model, Biophys. J 100 (2011) 2679–2687. [PubMed: 21641313]

[17]. Mijailovich S, Kayser-Herold O, Li X, Griffiths H, Geeves M, Cooperative regulation of myosin-s1 binding to actin filaments by a continuous flexible tm-tn chain, Eur Biophys J 41 (2012) 1015–1032. [PubMed: 23052974]

[18]. Metalnikova NA, Tsaturyan AK, A mechanistic model of ca regulation of thin filament in cardiac muscle, Biophys. J. 105 (2013) 941–950. [PubMed: 23972846]

[19]. Smith D, Path-integral theory of an axially confined work-like chain, J. Phys. Math. Gen 34 (2001) 4507–4523.

[20]. Behrmann E, Muller M, Penczek P, Mannherz H, Manstein D, Raunser S, Structure of the rigor actin-tropomyosin-myosin complex, Cell 150 (2) (2012) 327–338. [PubMed: 22817895]

[21]. Bacchiocchi C, Lehrer SS, Ca^{2+}-induced movement of tropomyosin in skeletal muscle thin filaments observed by multi-site fret, Biophys. J 82 (2002) 1524–1536. [PubMed: 11867466]

[22]. Holthauzen MFL, Correa F, Farah CS, Ca^{2+}-induced rolling of tropomyosin in muscle thin filaments: the alpha- and beta-band hypothesis revisited., J Biol Chem 279 (2004) 15204–15213. [PubMed: 14724287]

[23]. Sousa D, Stagg SM, Stroupe E, Cryo-em structures of the actin:tropomyosin transition from c-to-m-state, J. Mol. Biol 425 (2013) 4544–4555. [PubMed: 24021812]

[24]. Li XE, Tobacman L, Mun J, Craig R, Fischer S, Lehman W, Tropomyosin position on f-actin revealed by em reconstruction and computational chemistry, Biophys. J 100 (2011) 1005–1013. [PubMed: 21320445]

[25]. Lehman W, Orzechowski M, Li X, Fischer S, Raunser S, Gestalt-binding of tropomyosin on actin during thin filament activation, J Muscle Res Cell Motil 34 (2013) 155–163. [PubMed: 23666668]

[26]. Orzechowski M, Moore JR, Fischer S, Lehman W, Tropomyosin movement on f-actin during muscle activation explained by energy landscapes, Archives of Biochemistry and Biophysics 545 (2014) 63–68. [PubMed: 24412204]

[27]. Orzechowski M, Fischer S, Moore JR, Lehman W, Farman GP, Energy landscapes reveal the myopathic effects of tropomyosin mutations, Archives of Biochemistry and Biophysics 564 (2014) 89–99. [PubMed: 25241052]

[28]. Aboelkassem Y, Trayanova N, Tropomyosin dynamics during cardiac thin filament activation as governed by a multi-well energy landscape, Biophys J 110 (2016) 524a.

[29]. Julicher F, Force and motion generation in molecular motors: A generic description In Muller SC, Parisi J, Zimmermann W, editor. Transport and structure in biophysical and chemical phenomena, 1999.

[30]. Liebovitch LS, Czegledy FP, A model of ion channel kinetics based on deterministic, chaotic motion in a potential with two local minima, Ann. Biomed. Eng 20 (1992) 517–531. [PubMed: 1384403]

[31]. Loong CKP, Takeda AK, Badar MA, Rogers JS, Chase PB, Slowed dynamics of thin filament regulatory units reduces ca2+-sensitivity of cardiac biomechanical function, Cell Molec Bioeng 6 (2013) 183–198. [PubMed: 23833690]

[32]. Hui W, Shu Mao JMC, Marriott G, Tropomyosin dynamics in cardiac thin filaments: a multisite forster resonance energy transfer and anisotropy study, Biophys. J 94 (2008) 4358–4369. [PubMed: 18310249]

[33]. Melnikov VK, On the stability of the center for time-periodic perturbations, Trans. Moscow Math. Soc 12 (1963) 1–57.

[34]. Siewe MS, Tchawoua C, Rajasekar S, Homoclinic bifurcations and chaos in ϕ^6 - rayleigh oscillator with three wells drived by amplitude modulated force, Int. J. Bifurcation and Chaos 21 (2011) 1583–1593.

[35]. Ischii Y, Lehrer SS, Two-site attachment of troponin to pyrenelabelled tropomyosin, J Biol Chem 266 (1991) 6894–6903. [PubMed: 2016303]

[36]. Lehman W, Vibert P, Uman P, Craig R, Steric blocking by tropomyosin visualised in relaxed vertebrate muscle thin filaments, J Mol Biol 251 (1995) 191–196. [PubMed: 7643394]

[37]. Xu C, Craig R, Tobacman L, Horowitz R, Lehman W, Tropomyosin positions in regulated thin filaments revealed by cryoelectron microscopy, Biophys. J. 77 (1999) 985–992. [PubMed: 10423443]

[38]. Brown JH, Kim KH, Jun G, Greenfield NJ, Dominguez R, Volkmann N, Hitchcock-DeGregori SE, Cohen C, Deciphering the design of the tropomyosin molecule, Proc Natl Acad Sci 98 (2001) 8496–8501. [PubMed: 11438684]

[39]. Greenfield NJ, Huang YJ, Palm T, Swapna GV, Monleon D, Montelione GT, Hitchcock-DeGregori SE, Solution nmr structure and folding dynamics of the n terminus of a rat non-muscle alpha-tropomyosin in an engineered chimeric protein, J Mol Biol 312 (2001) 833–847. [PubMed: 11575936]

[40]. Brown JH, Zhou Z, Reshetnikova L, Robinson H, Yammani RD, Tobacman LS, Cohen C, Structure of the mid-region of tropomyosin: bending and binding sites for actin, Proc Natl Acad Sci 102 (2005) 18878–83. [PubMed: 16365313]

[41]. Holmes KC, Lehman W, Gestalt-binding of tropomyosin to actin filaments, J Muscle Res Cell Motil. 29 (2008) 213–219. [PubMed: 19116763]

[42]. Greenfield NJ, Huang YJ, Swapna GV, Bhattacharya A, Rapp B, Hitchcock-DeGregori SE, Solution nmr structure of the junction between tropomyosin molecules: implications for actin binding and regulation, J Mol Biol 364 (2006) 80–96. [PubMed: 16999976]

[43]. Sousa D, Cammarato A, Jang K, Graceffa P, Tobacman LS, Li XE, Lehman W, Electron microscopy and persistence length analysis of semi-rigid smooth muscle tropomyosin strands, Biophys. J. 99 (2010) 862–868. [PubMed: 20682264]

[44]. Miki M, Makimura S, Saitoh T, Bunya M, Sugahara Y, Ueno Y, Kimura-Sakiyama C, Tobita H, A three-dimensional fret analysis to construct an atomic model of the actin-tropomyosin complex on a reconstituted thin filament, J Biol Chem 414 (2011) 765–782.

[45]. Barua B, Fagnant PM, Winkelmann DA, Trybus KM, Hitchcock-DeGregori SE, A periodic pattern of evolutionarily conserved basic and acidic residues constitutes the binding interface of actin-tropomyosin, J Biol Chem 288 (2013) 9602–9609. [PubMed: 23420843]

[46]. von der Ecken J, Mu M, Lehman W, Manstein DJ, Penczek PA, Raunser S, Structure of f-actin-tropomyosin complex, Nature 519 (2015) 114–7. [PubMed: 25470062]

[47]. Wegner A, Equilibrium of the actin-tropomyosin interaction, J Mol Biol 131 (1979) 839–853. [PubMed: 513132]

[48]. Greenfield N, T. P,Hitchcock-DeGregori SE, Structure and interactions of the carboxyl terminus of striated muscle α-tropomyosin: It is important to be flexible, Biophys. J. 83 (2002) 2754–2766. [PubMed: 12414708]

[49]. Singh A, Hitchcock-DeGregori S, Local destabilization of the tropomyosin coiled coil gives the molecular flexibility required for actin binding, Biochemistry 42 (2003) 14114–14121. [PubMed: 14640678]

[50]. Bivin D, Stone D, Schneider D, Mendelson R, Cross-helix separation of tropomyosin molecules in acto-tropomyosin as determined by neutron scattering, Biophys. J. 59 (1991) 880–888. [PubMed: 1829644]

[51]. Narita A, Yasunaga T, Ishikawa T, Mayanagi K, Wakabayashi T, Ca^{2+}-induced switching of troponin and tropomyosin on actin filaments as revealed by electron cryo-microscopy1, J Mol Biol 308 (2001) 241–261. [PubMed: 11327765]

[52]. Lehman W, Craig R, Vibert P, Ca^{2}+-induced tropomyosin movement in limulus thin filaments revealed by three-dimensional reconstruction, Nature 368 (1994) 65–67. [PubMed: 8107884]

[53]. Pirani A, Xu C, Hatch V, Craig R, Tobacman L, Lehman W, Single particle analysis of relaxed and activated muscle thin filaments, J Mol Biol 346 (2005) 761–772. [PubMed: 15713461]

[54]. Campbell SG, Lionetti FV...., McCulloch AD, Coupling of adjacent tropomyosins enhances cross-bridge-mediated cooperative activation in a markov model of the cardiac thin filament, Biophys J 98 (2010) 2254–2264. [PubMed: 20483334]

[55]. Aboelkassem Y, Bonilla JA...., Campbell S, Contributions of ca^{2+} -independent thin filament activation to cardiac muscle function, Biophys J 109 (2015)2101–2112. [PubMed: 26588569]

[56]. Aboelkassem Y, McCabe KJ, Huber G, Sundnes J, McCulloch AD, Turning the azimuthal motions of adjacent tropomyosins into a coupled n-body problem in a brownian model of cardiac thin filament activation, Biophys J 114 (2018) 502a–503a.

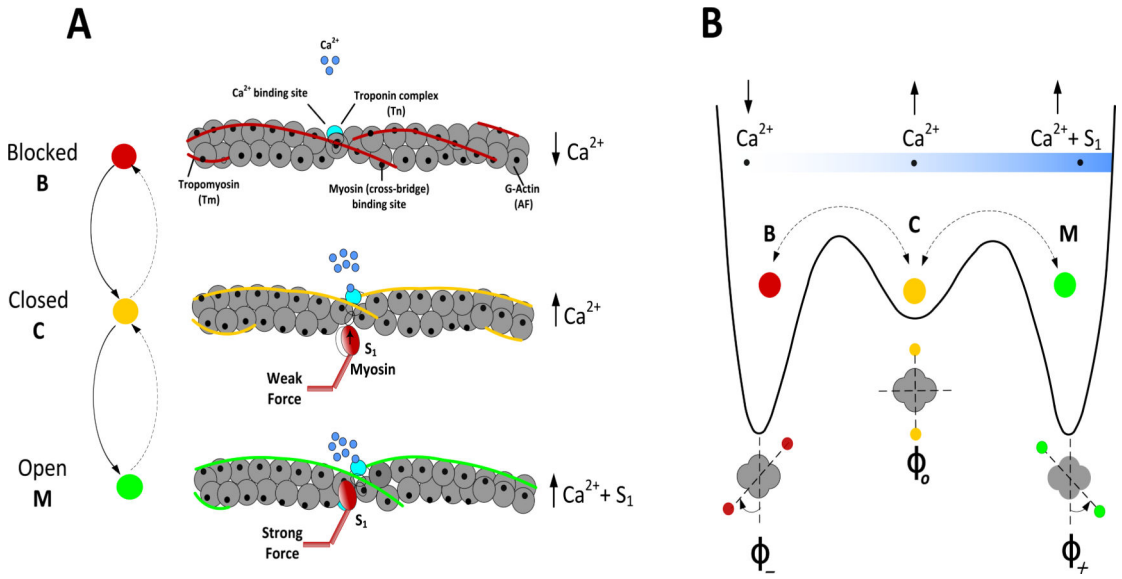

Figure 1:

Schematic diagram of the model components and tropomyosin transition states as described by an energy landscape profile during muscle activation. (A) The structure of myofilament main components and tropomyosin's regulatory positions. (B) Tropomyosin dynamics as governed by a multi-well potential mimicking the three-state (B, C, M) model.

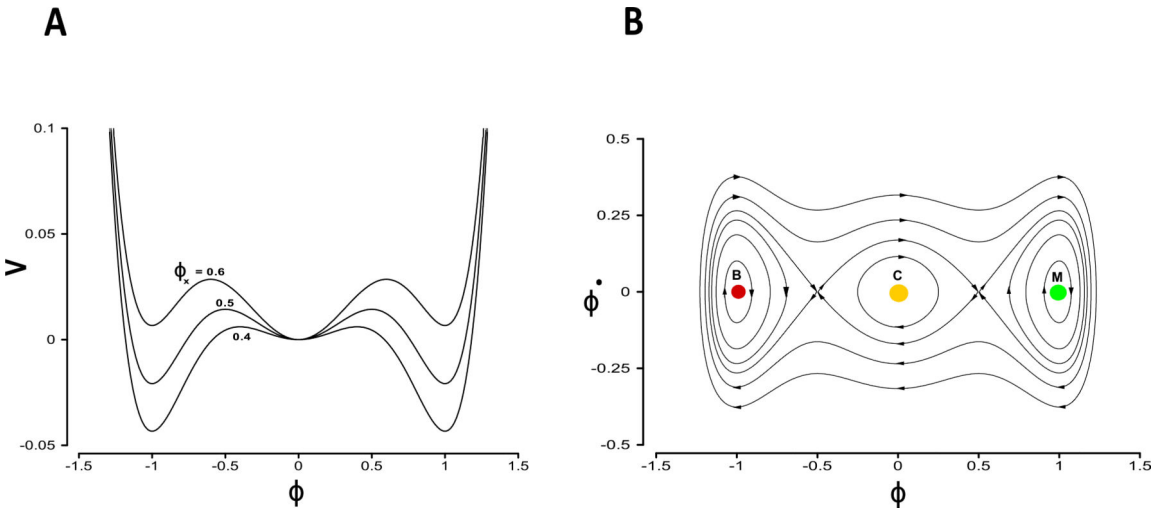

Figure 2:

The energy landscape profile with a multi-well topology proposed to govern tropomyosin dynamics in the azimuthal direction (ϕ): (A) The effect of saddle point locations (ϕ_χ) on the potential profile. (B) Phase portrait for the unforced and undamped Tm dynamical system along with its stable (B-C-M) conformational states.

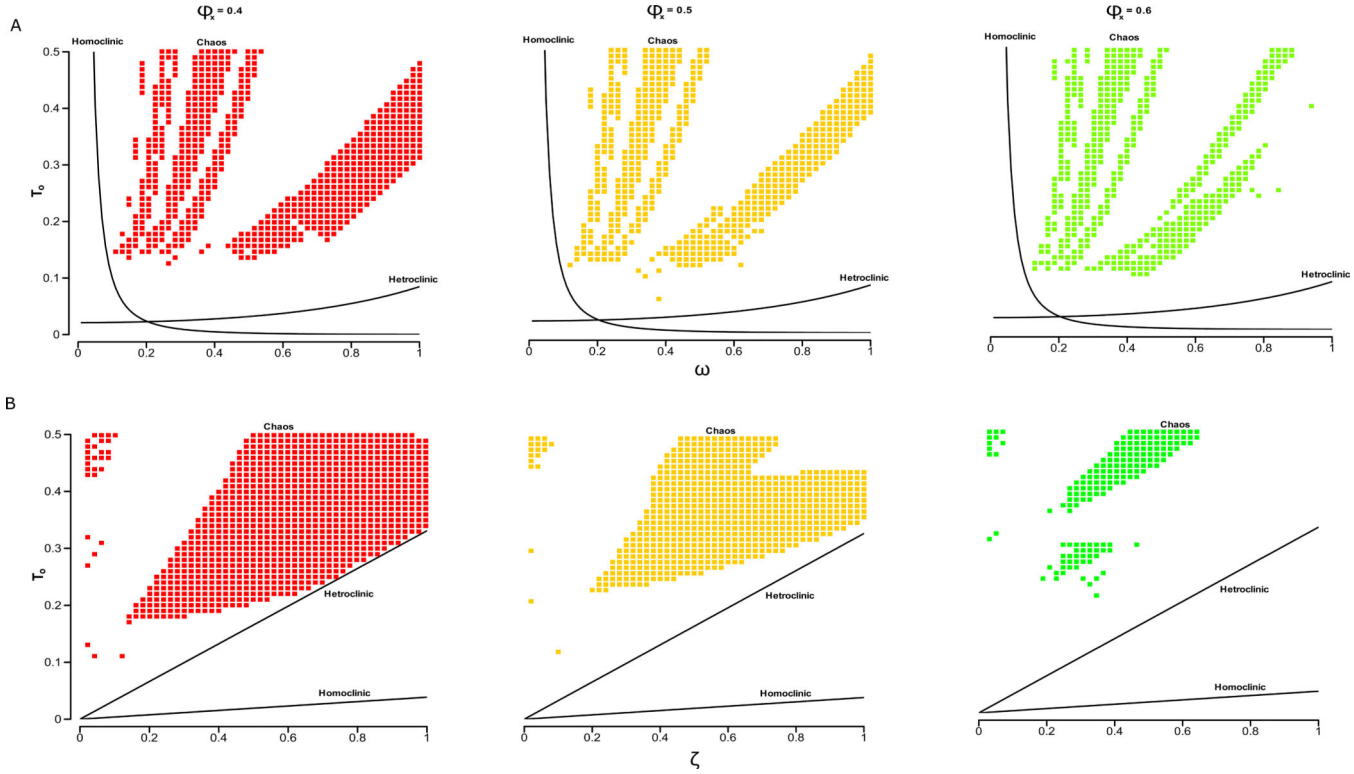

Figure 3:

Analytical and numerical simulations that show parameter ranges where chaotic behavior can occurs for various values of ϕ_x = 0.4, 0.5, and 0.6 respectively. Conditions from the bifurcation analysis for both homoclinic and heteroclinic orbits are obtained analytically using Melnikov function and are represented by the solid lines. The "+" signs refer to chaotic conditions that were obtained numerically. Simulations were performed with Tm positioned initially in the closed "C"-state: (A) The frequency-amplitude plane (ω - T_o) at ζ = 0.3. (B) The damping-amplitude plane (ζ - T_o) at ω = 0.75.

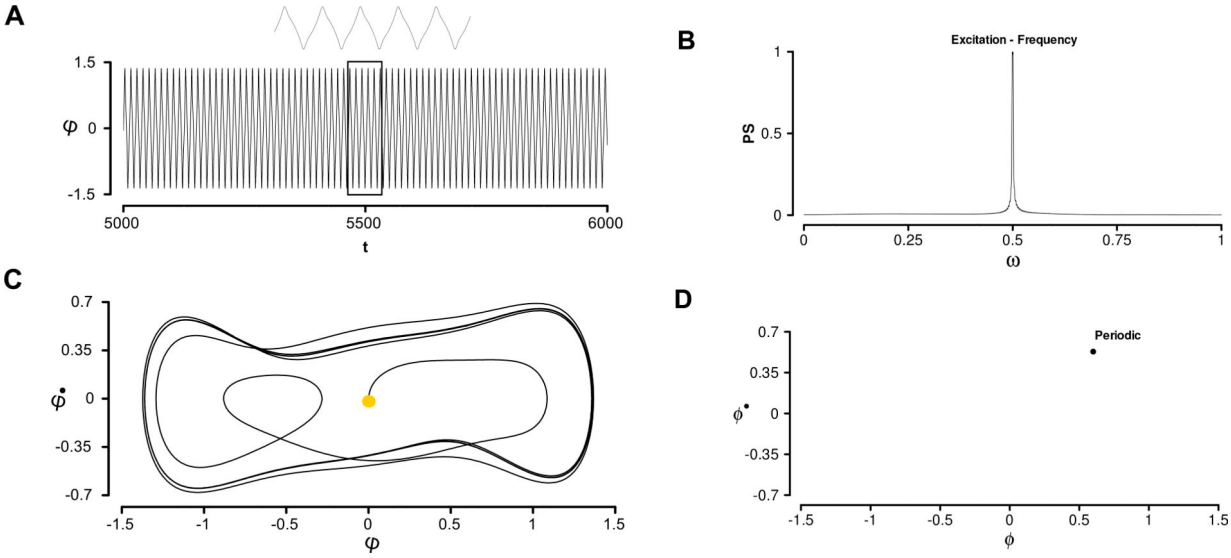

Figure 4:

Periodic response exhibited by Tm movements over the surface of actin filament. In this particular scenario, Tm molecules behave as simple harmonic oscillators during striated muscle activation. Results shown herein are obtained for values ω= 0.5, ζ = 0.3, and T_o = 0.1. These parameters were chosen based on conditions obtained previously and shown in Fig. 3: (A) Tm's angular positions over multiple cycles after ignoring transient response. (B) Frequency response of the time series obtained using Fourier analysis; it shows that Tm moves with a frequency similar to the excitation frequency. (C) Phase portrait demonstrating that Tm converges to limit cycle oscillations. (D) The Poincare' map showing that periodic (i.e., period-1) response indeed occurs.

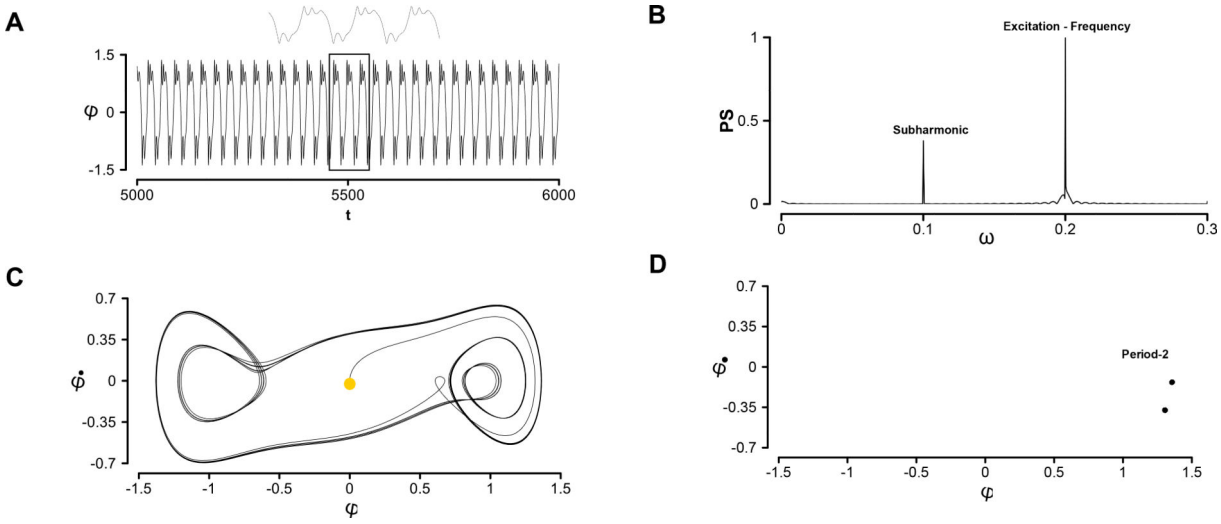

Figure 5:

Period-2 response, where Tm oscillates with two frequencies. Parameters for this scenario were found numerically as ω= 0.2, ζ = 0.3, and T_o = 0.24. A) Tm's angular positions over many cycles. (B) Frequency response showing that Tm can oscillate with two (fundamental and super-harmonic) frequencies. (C) Phase portrait shows that Tm could move between regulatory states with two frequencies. (D) The Poincare' map have two points only, confirming the existence of period-2 behavior.

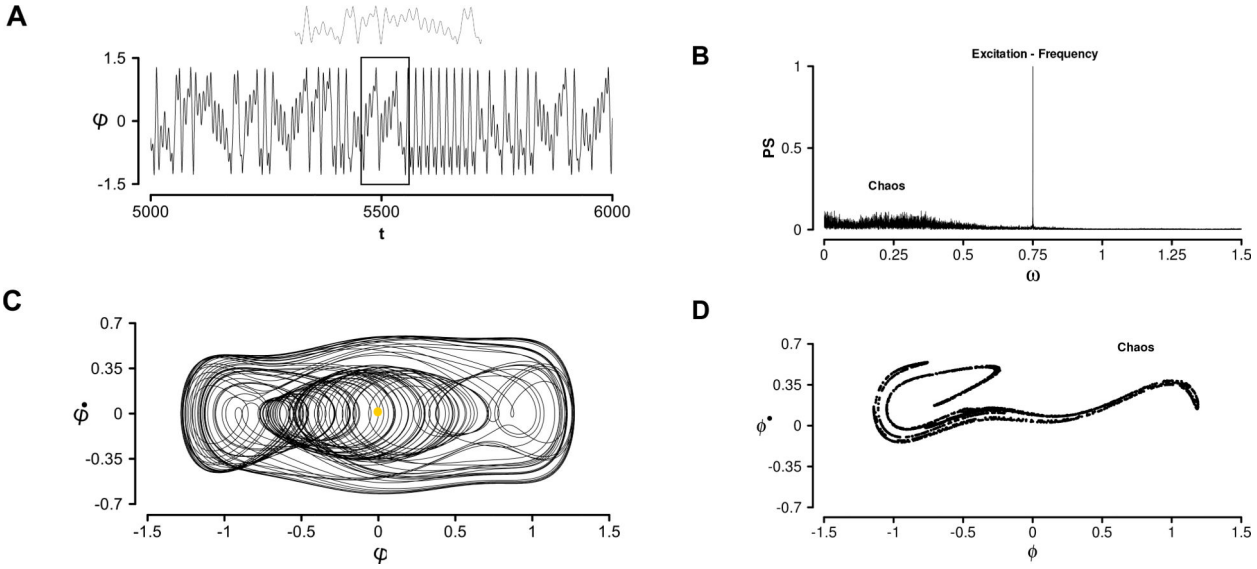

Figure 6:

Chaotic response, where Tm can oscillate with complex patterns (Yet, it is not a random motion) due to the system nonlinearity. Its dynamical response is so sensitive to initial conditions and to any small perturbations. Parameters for this scenario were found numerically ω= 0.75, $\zeta = 0.3$, and $T_o = 0.24$: (A) Tm's angular positions over many cycles. (B) Frequency response showing that multiple frequencies are involved in the Tm motions. (C) Phase portrait demonstrating that Tm could move chaotically between regulatory states. (D) The Poincare' map have many points that are distributed in a "horseshoe" pattern, which indicating the existence of chaotic responses.

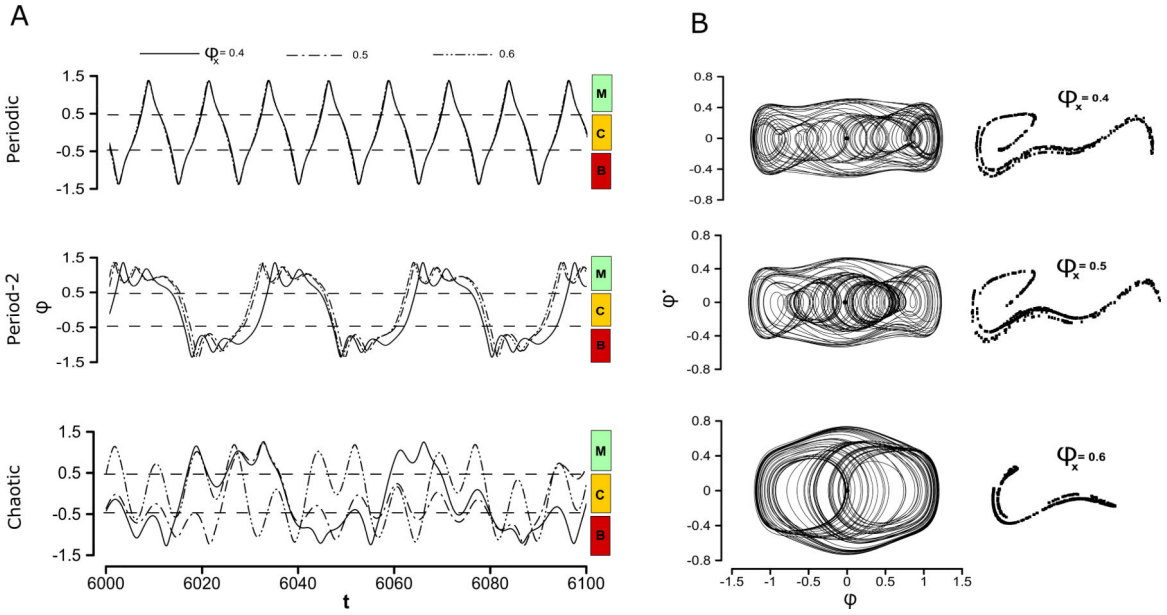

Figure 7:

The effects of ϕ_x on Tm dynamical responses as it alternates between equilibrium positions: (A) The Tm's azimuthal position as a function of the simulated time during periodic, period-2, and chaotic cases. (B) The phase portrait and the Poincare' maps for the chaotic case only.

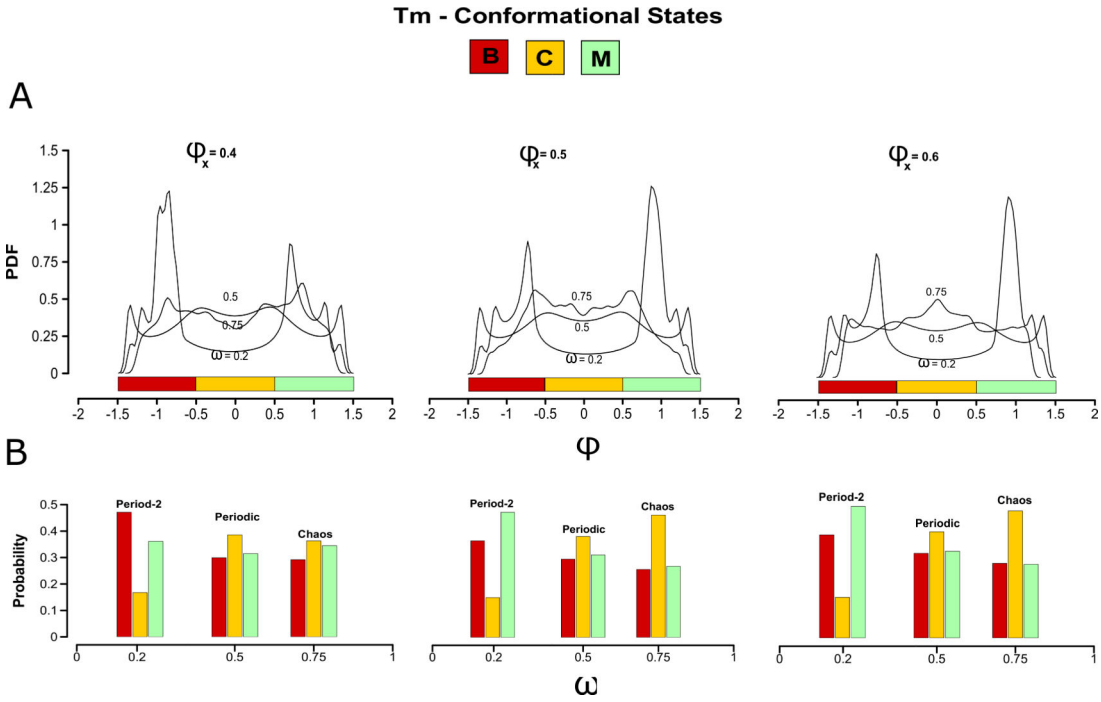

Figure 8:

Tm residence times in each state as measured by the probability distribution functions (PDF) for various values of ϕ_X = 0.4, 0.5, and 0.6 respectively. Results are given for the periodic (ω = 0.5), period-2 (ω = 0.2), and chaotic (ω = 0.75) cases: (A) The probability distribution functions (averaged over entire cycles) show occupancy by each conformational (B,C,M) state. (B) The probability for each state calculated by integrating each probability distribution function over the corresponding range.

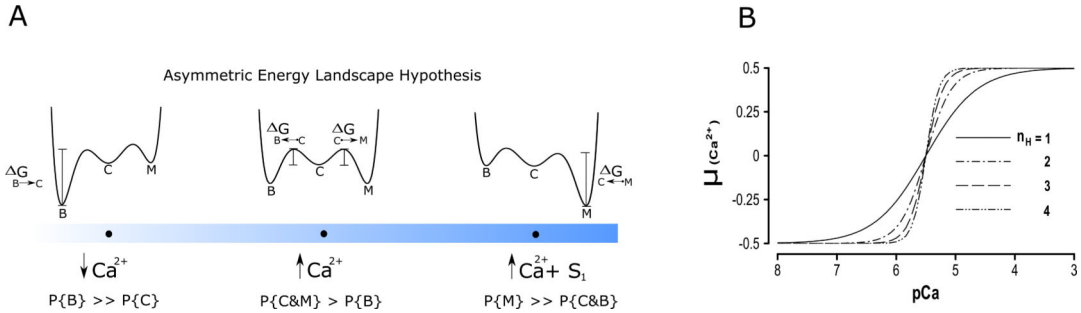

Figure 9:

Hypothetical asymmetric energy landscape as a function of Ca-concentrations: (A) A schematic showing how the energy potential varies as Ca^{2+} increases during thin filament activation along with the probability of being in one of the conformational (B,C,M) states. (B) A Hill-like activation coefficient $\mu(Ca^{2+})$ as a function of pCa levels for different Hill's indexes, used to introduce asymmetry in the energy landscape profile.

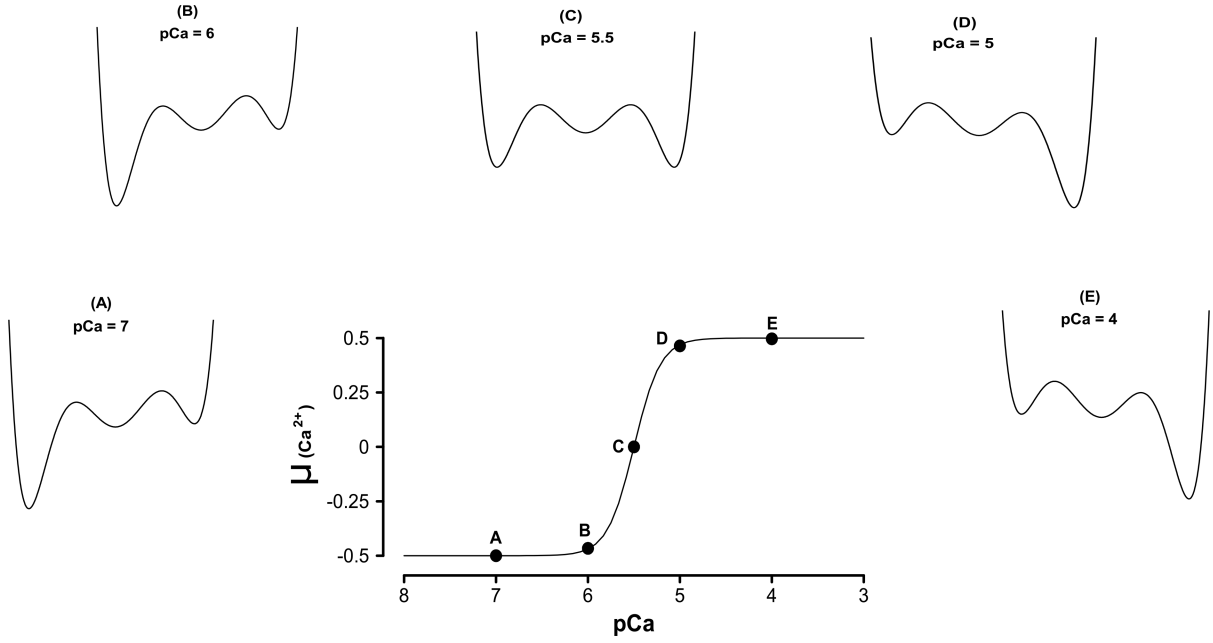

Figure 10:

The Ca^{2+}-dependency of the modified energy potential $V_{\mathrm{Asym}}(\phi)$ to account for the asymmetry characteristics that are needed for a realistic thin filament activation. Profiles are calculated at different values of pCa i.e., at different values of the activation coefficient μ. Asymmetry is biased toward B-sate and M-state at lower and high Ca^{2+} levels respectively. This asymmetry is relaxed at moderate Ca^{2+} levels mimicking the C-sate. A pure symmetric energy profile can be recovered at $\mu = 0.5$ i.e., pCa=5.5 i.e., at half activation.